

PROCEEDINGS OF SPIE

SPIDigitalLibrary.org/conference-proceedings-of-spie

Fractal analysis for classification of breast lesions

L. B. Alvarado-Cruz, M. Delgadillo-Herrera, C. Toxqui-Quitl, A. Padilla-Vivanco, R. Castro-Ortega, et al.

L. B. Alvarado-Cruz, M. Delgadillo-Herrera, C. Toxqui-Quitl, A. Padilla-Vivanco, R. Castro-Ortega, M. Arreola-Esquivel, "Fractal analysis for classification of breast lesions," Proc. SPIE 11104, Current Developments in Lens Design and Optical Engineering XX, 111040U (30 August 2019); doi: 10.1117/12.2531201

SPIE.

Event: SPIE Optical Engineering + Applications, 2019, San Diego, California, United States

Fractal analysis for classification of breast lesions

L. B. Alvarado-Cruz ^a, M. Delgadillo-Herrera^a, C. Toxqui-Quitl^a, A. Padilla-Vivanco^a, R. Castro-Ortega ^a, and M. Arreola-Esquivel^a

^aComputer Vision Laboratory, Universidad Politécnica de Tulancingo, Ingenierías 100, Huapalcalco, 43629, México.

ABSTRACT

Nowadays, breast lesions are a common health problem among women. Breast thermograms are images recorded by digital-optical systems with high resolution that use infrared technology in order to show vascular and temperature changes. In the present work, we study benign and malignant breast lesions shape by means of fractal analysis. The Fractal Dimension (FD) is calculated with the Box Counting method and the Hurst exponent is obtained using the Wavelet coefficients and the Detrending Moving Average algorithm. These algorithms was applied to synthetic images and breast thermograms. The Fractal Dimension value is used for patient classification with or without breast injury. The proposed methodology was applied to the Database For Mastology Research (DMR) in order to classify thermographic images. The FD of ROIs for breast thermograms was calculated. Results shows that the FD BCM values ranges from [0.45,0.81] in 4 healthy cases and from [0.92,1.33] in 4 unhealthy cases.

Keywords: Fractal analysis, breast thermograms, breast lesions.

1. INTRODUCTION

In recent years, breast cancer has been a relevant health problem that shows growing trend in both incidence and early diagnosis¹. The main characteristic of this condition is the rapid and disorganized growing trend of abnormal cells. This process causes an exponential increase of the temperature in tissue². Thermal symmetry and asymmetry caused by normal and abnormal cells can be analyzed through the use of infrared images,^{3,4}. Moreover metabolic activity and vascular circulation can be also studied through of this kind of images⁵. Abnormal cells show a chaotic and poorly regulated growth. They also show an irregular morphology that can not be measured by classic Euclidean geometry based on shapes such as lines or spheres⁶. Computer-Aided Detection (CAD) systems based on the analysis of breast thermograms can be used to help us in order to identify abnormal thermal patterns related with possible breast cancer⁷.

Several studies have shown that by fractal geometry, an irregular shape, can be useful to quantitatively describe the morphology of tumors⁶. James W. et al., describes mathematical models known as statistical growth processes and the application fractals to cancer as morphometric tools for diagnostic and prognostic purposes.⁸. According to Katharina Klein et al., they use fractal analysis to identify malignant cells in microscopic images by reflection interference contrast of individual living cells⁹. On the other hand, Maryam Arab Zade et al., indicate that the Fractal Dimension (FD) allows to differentiate malignant or benign tumors in the breast in a quantitative way¹⁰. Anindita et al., research the efficacy of fractal characteristics for the discrimination of abnormal and normal breast images in mammography and breast thermography¹¹. In this work, we calculate the Fractal Dimension and the Hurst exponent of the maximum temperature regions in breast thermograms. The paper is organized as follows. In Section 2 we describe the mathematical methods to calculate the Fractal Dimension and Hurst exponent. Section 3 presents the numerical analysis using synthetic images. The fractal analysis of the breast thermograms are given in Section 4. Finally, in Section 5 the conclusions are summarized.

Further author information: (Send correspondence to L.B. Alvarado-Cruz.)
A.A.A.: laura.alvarado.1631026@upt.edu.mx., Telephone: (+52) 7761155738

2. METHODS FOR CALCULATE THE FRACTAL DIMENSION AND THE HURST EXPONENT

The fractal geometry analysis was first introduced by Mandelbrot in 1975 in order to study the irregular surfaces found in nature as tree leaves, snowflakes, and among others¹². The main characteristics of a fractal are: self-similarity and fractal dimension. Different methods have been proposed to calculate the fractal dimension and the Hurst Exponent (H), some of them are analyzed below.

2.1 Box Counting Method (BCM)

This algorithm is very common to measure the fractal dimension of the objects contour¹³. The basic mathematical form is,

$$N(r) = Cr^{-FD}, \quad (1)$$

where $N(r)$ is the number of boxes that cover the perimeter of the image, C is a constant, r is the size of the side of each square box and D is the fractal dimension. Thus, FD, for a given r , of the object is defined as¹⁴,

$$FD = \frac{\log(N(r))}{\log(\frac{1}{r})}. \quad (2)$$

To obtain the FD of the object, it is necessary to graph $\log N(r)$ vs $\log(1/r)$ and the slope of the line that best fitting the data is the FD¹⁵. Figure 1 shows an irregular sample contour and its respective Fractal dimension.

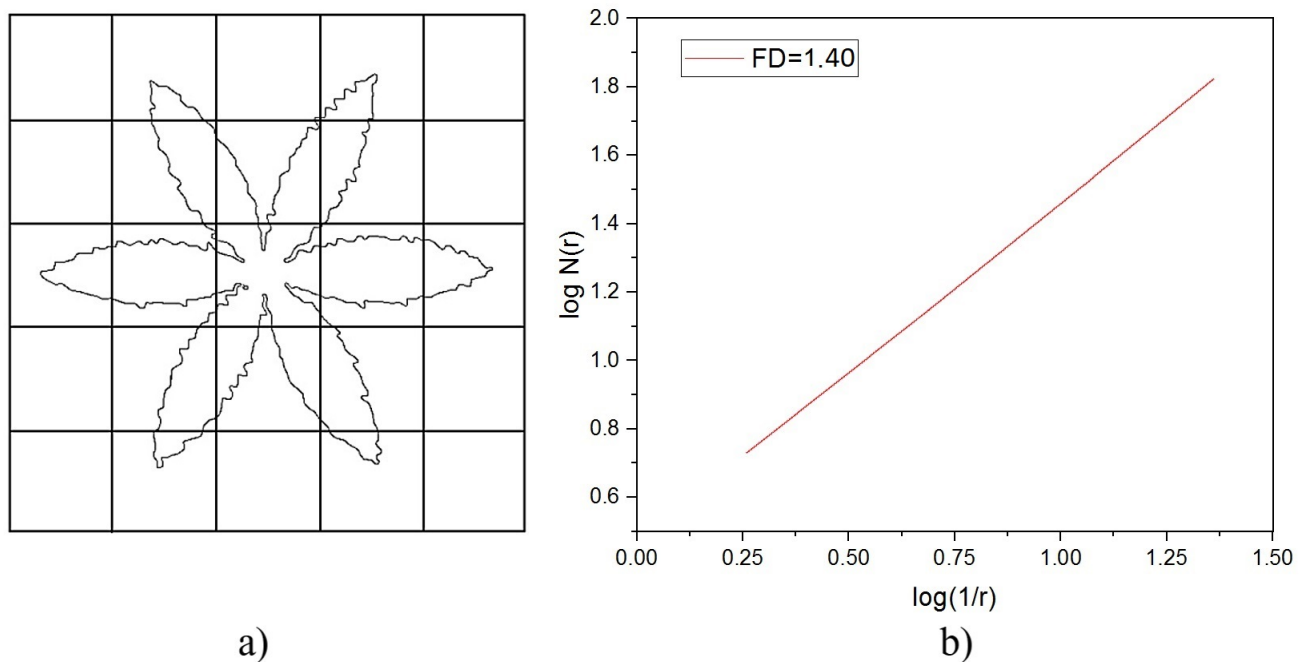


Figure 1: Calculation of the fractal dimension of an irregular contour shape by the Box Counting method. a) Sampling of a rough shape. In this case $N(r) = 15$ and $1/r=5$. The slope of the line in b) is a measure of the fractal dimension FD.

2.2 Detrending Moving Average (DMA)

For a *two-dimensional* image $f(i, j)$ of size $N \times M$ the generalized variance is defined by,

$$\sigma_{DMA}^2 = \frac{1}{(N - n_{max})(M - m_{max})} \sum_{i=n-u}^{N-u} \sum_{j=m-v}^{M-v} [f(i, j) - \tilde{f}_{n,m}(i, j)]^2, \quad (3)$$

with $\tilde{f}_{n,m}$ given by,

$$\tilde{f}_{n,m} = \frac{1}{nm} \sum_{i=k=-u}^{n-1-u} \sum_{l=-v}^{m-1-v} f(i-k, j-l), \quad (4)$$

where n is the sliding window $n_{max} = \max(n) \ll N$, $m_{max} = \max(M) \ll M$, u and v are determinate by $u = \text{int}(n \cdot \theta_1)$ and $v = \text{int}(m \cdot \theta_2)$, respectively. And $\theta_1, \theta_2 \in [0,1]$ ¹⁶. The variance obtained at each subarray is plotted as a function of $s = m \times n$ on $\log - \log$ axes; the slope of the regression line corresponds to the Hurst exponent.

2.3 Wavelet coefficients (WC)

The Wavelet coefficients can reflect the information of the spatial-frequency image content. Thus, Wavelet coefficients of a real function $f(x, y)$ can be defined as,

$$C_{m,n} = \frac{1}{\sqrt{m}} \sum_x \sum_y f_{x,y} \psi_{m,n} \left(\frac{x-n}{m}, \frac{y-n}{m} \right). \quad (5)$$

where $\psi_{m,n}$ is the basic Wavelet. For a given scale m , the energy of coefficients at that scale are,

$$\Gamma_m = \frac{1}{\sqrt{n_m}} \sum_{n \in \mathbb{Z}} |C_{m,n}|^2. \quad (6)$$

Γ_m is now the energy of the Wavelet coefficients at scale m , n_m is the number of coefficients at scale m ¹⁷.

$$\Gamma_m = 2^{m(\gamma)} \Gamma_0 \quad (7)$$

where $\gamma = 2H + 1$ and $0 < H < 1$.

The energy obtained at each scale is plotted on $\log - \log$ axes; the slope of the regression line corresponds to the Hurst exponent. The Hurst exponent value is related with the FD as,

$$FD = 2 - H \quad (8)$$

3. NUMERICAL ANALYSIS USING SYNTHETIC IMAGES

In this section, we present the numerical analysis using synthetic images. We use shapes with smooth and rougher contours as show in Figs. 2. In the first set of Table 1, the binary images (a-f) have smooth and rough contours. The box counting method described in section 2.1 applies to this data set. The FD BCM obtained for image a) is smaller than that corresponding to image b). This is because the shape of the image a) is softer than the shape of image b). A similar behavior of the FD BCM is obtained for the shapes c-d and e-f. For the Hurst exponent extraction, two different methods are used: the DMA and the WC. As we can see, the value of the Hurst exponent (H DMA) corresponds to the morphology of the forms. The H DMA obtained for image a) is bigger than that corresponding to image b). This is because the shape of the image a) is softer than the shape of image b). A similar behavior of the H DMA is obtained for the shapes c-d and e-f. In a similar way, the H WC obtained for image a) is bigger than that corresponding to image b). Table 2 shows the FD and H values obtained from the edge images of Table 1. The best results were obtained from images such as those in Table 1. The values highlighted in red do not correspond to the type of morphology analyzed. Therefore, the FD and H are calculated for the binary images of the ROI in thermograms, not for its edges.

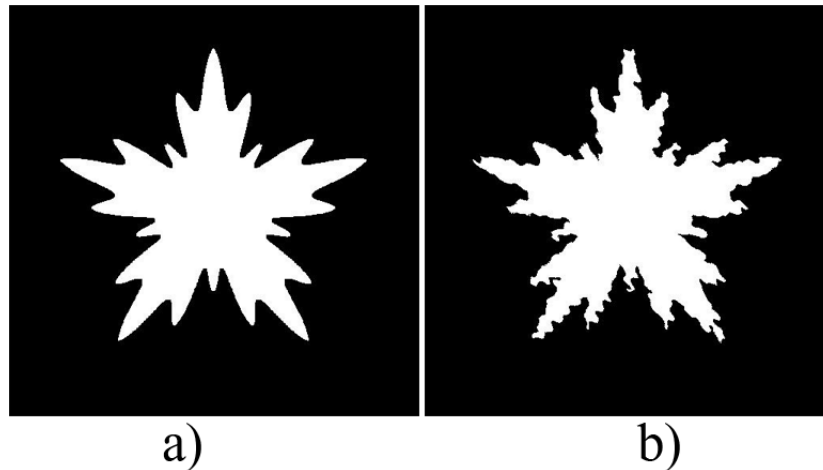


Figure 2: Shape with a) Smooth and b) Roughness contours.

Table 1: Calculated FD and H values for the binary image smooth (a) and rougher (b) shape.

Shape	a)	b)	c)	d)	e)	f)
FD BCM	1.34219	1.36556	1.30733	1.32525	1.23158	1.2664
H DMA	0.32663	0.30295	0.16742	0.15135	0.43383	0.33413
H WC	0.3837	0.38295	0.38435	0.38399	0.37304	0.3724

Table 2: Calculated FD and H values edge from binary image for the smooth(a) and rougher (b) shape.

Shape	a)	b)	c)	d)	e)	f)
FD BCM	0.86048	0.67788	0.69267	0.67475	0.76842	0.73351
H DMA	0.086055	0.086605	0.21407	0.2168	0.13775	0.12693
H WC	1.70926	0.2795	0.16261	0.14812	0.204	0.19107

4. FRACTAL ANALYSIS OF BREAST THERMOGRAMS

According to the literature, malignant and benign cells show fractal characteristic patterns. The morphological analysis of cells by fractals can be used to differentiate between one case or another. We studied 8 breast thermograms available in the public database of Visual Lab of the Federal Fluminense University of Brazil¹⁸. Hence, we have 4 labeled as unhealthy and 4 labeled as healthy. The study is based on the analysis of the hottest regions. A 2D surface of temperature increases are obtained by Alvarado et al.³, and extraction of the ROI by Zermeno et al.,⁴ The Figs. 3a and 3b shows a thermogram labeled as healthy it is represented represented by

increases in temperature. The ROI and their edge of the hottest region is shows in Figs. 3c and 3d. In the same way, Figs. 4a and 4b shows a thermogram labeled as unhealthy.

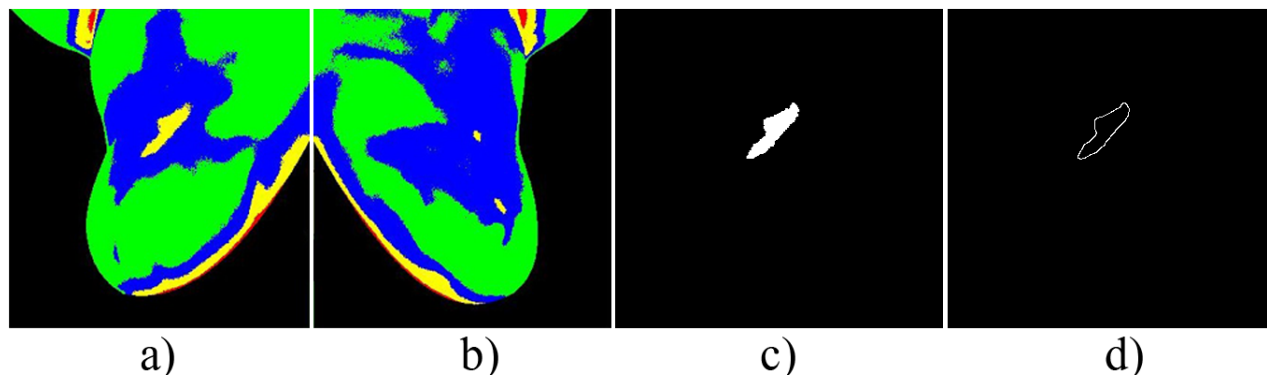


Figure 3: Thermogram labeled as healthy represented by increases in temperature. a) Right breast. b) Left breast. c) Hottest ROI. d) Boundary contours of the hottest ROI $\Delta_{tmax} = 1.9763$.

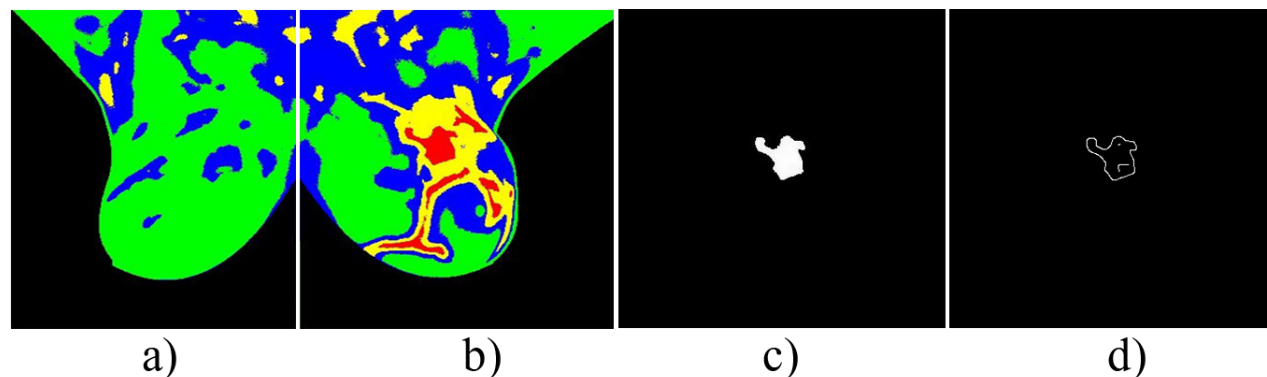


Figure 4: Thermogram labeled as unhealthy represented by increases in temperature. a) Right breast. b) Left breast. c) Hottest ROI. d) Boundary contours of the hottest ROI $\Delta_{tmax} = 4.06$.

The ROI of breast thermography images is characterized by fractal analysis. This values are shown in Table 3. The FD BCM from healthy thermogram ranges [0.45, 0.81] and from a unhealthy case it ranges [0.92, 1.33]. This value can significantly difference between both cases.

Table 3: Values of FD of breast thermograms.

Case	h1	h2	h3	h4	u1	u2	u3	u4
FD BCM	0.606	0.645	0.454	0.8133	0.988	0.921	1.266	1.333

A feature vector that describes the ROI of a thermogram, is defined as $d1 = [Area, \Delta_{tmax}, FD\ BCM]$. These features are obtained from 16 breast thermograms. The results of Fig. 5 clearly show that the descriptors allow to differentiate between unhealthy and healthy breast thermograms. In a similar way, the Fig. 6 shows the results obtained by means of a feature vector $d2 = [FD\ BCM, H\ DMA, H\ WC]$ from 16 breast thermograms. These results allow to identify malignancy and benign cases.

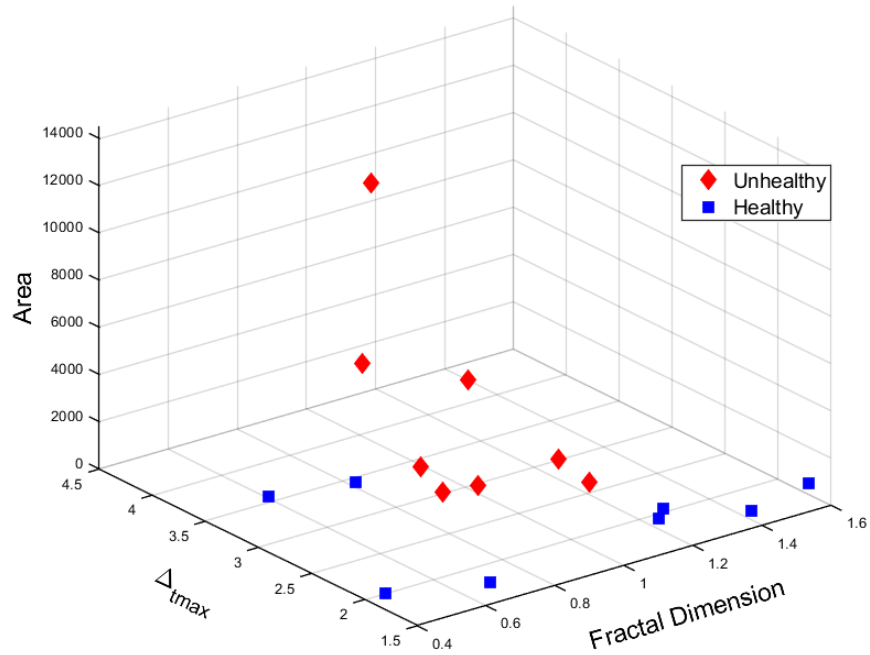


Figure 5: Three dimensional feature space applied to the ROI of 16 breast thermographic images. A feature vector is composed by $d1 = [Area, \Delta t_{max}, FD BCM]$.

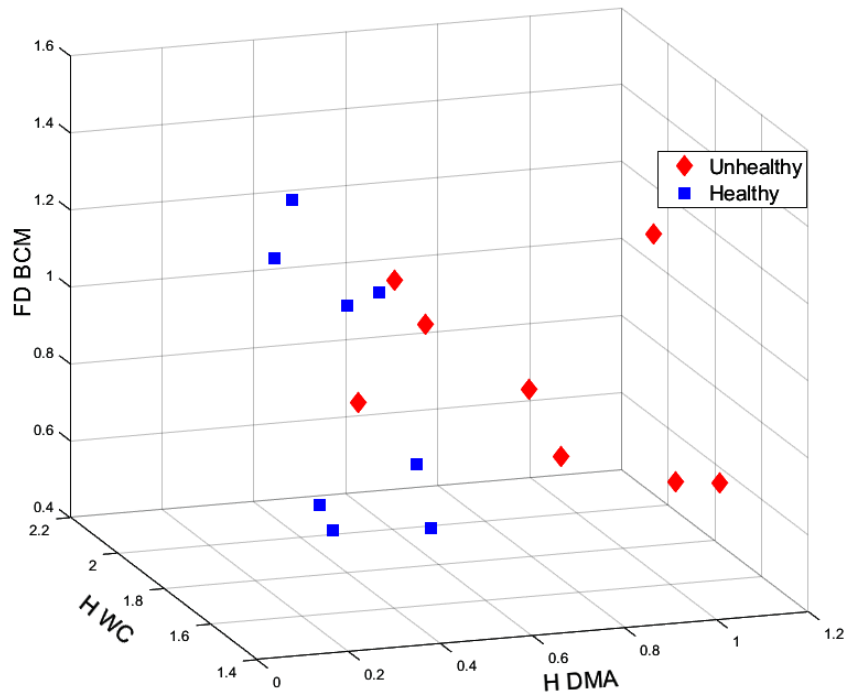


Figure 6: Three dimensional feature space applied to the ROI of 16 breast thermographic images. A feature vector is composed by $d2 = [FD BCM, H DMA, H WC]$.

5. CONCLUSIONS

In this paper we characterize the ROIs of breast thermograms by means fractal analysis. First, we present the numerical analysis using synthetic images. The values of FD and H are congruent with the morphology of the objects. As it was shown in the Tables 1 and 2. Next, eight images from the DMR database were analyzed. The results in Table 3 show that, the FD BCM values ranges from [0.45,0.81] in 4 healthy cases and from [0.92,1.33] in 4 unhealthy cases. The results obtained by means of features vectors $d1 = [\text{Area}; \text{tmax}; \text{FD BCM}]$ and $d2 = [\text{FD BCM}, \text{H DMA}, \text{H WC}]$ that describes the ROI from 16 breast thermograms showed in the Figs. 5 and 6 allow to identify malignancy and benign cases.

ACKNOWLEDGMENTS

The author would like to thank the Consejo Nacional de Ciencia y Tecnología (CONACyT) for the scholarship number 786815.

REFERENCES

- [1] Salinas-Martínez, A. M., Juárez-Ruiz, A., Mathiew-Quirós, Á., Guzmán-de la Garza, F. J., Santos-Lartigue, A., and Escobar-Moreno, C., “Cáncer de mama en México: tendencia en los últimos 10 años de la incidencia y edad al diagnóstico,” *Revista de Investigación Clínica* **66**(3), 210–217 (2014).
- [2] Ahmed, E., “Fractals and chaos in cancer models,” *International journal of theoretical physics* **32**(2), 353–355 (1993).
- [3] Alvarado-Cruz, L., Toxqui-Quitl, C., Hernández-Tapia, J., and Padilla-Vivanco, A., “Breast thermography: a non-invasive technique for the detection of lesions,” in [*Applications of Digital Image Processing XLI*], **10752**, 1075230–8, International Society for Optics and Photonics (2018).
- [4] Orozco-Guillén, E. and Zermeño-Loreto, O., “Caracterización de imágenes en la región espectral del infrarrojo para la detección de lesiones en mama,” **6**, 75–82 (2017).
- [5] Lavanya, A., “An approach to identify lesion in infrared breast thermography images using segmentation and fractal analysis,” *International Journal of Biomedical Engineering and Technology* **19**(3), 220–229 (2015).
- [6] Etehad Tavakol, M., Lucas, C., Sadri, S., and Ng, E., “Analysis of breast thermography using fractal dimension to establish possible difference between malignant and benign patterns,” *Journal of Healthcare Engineering* **1**(1), 27–43 (2010).
- [7] Li, Q. and Nishikawa, R., [*Computer-Aided Detection and Diagnosis in Medical Imaging*], Imaging in Medical Diagnosis and Therapy, CRC Press (2015).
- [8] Baish, J. W. and Jain, R. K., “Fractals and cancer,” *Cancer research* **60**(14), 3683–3688 (2000).
- [9] Klein, K., Maier, T., Hirschfeld-Warneken, V. C., and Spatz, J. P., “Marker-free phenotyping of tumor cells by fractal analysis of reflection interference contrast microscopy images,” *Nano letters* **13**(11), 5474–5479 (2013).
- [10] Zade, M. A. and Khodadadi, H., “Fuzzy controller design for breast cancer treatment based on fractal dimension using breast thermograms,” *IET systems biology* **13**(1), 1–7 (2018).
- [11] Roy, A., Gogoi, U. R., Das, D. H., and Bhowmik, M. K., “Fractal feature based early breast abnormality prediction,” in [*2017 IEEE Region 10 Humanitarian Technology Conference (R10-HTC)*], 18–21, IEEE (2017).
- [12] Mandelbrot, B., [*La geometría fractal de la naturaleza*], Libros para pensar la ciencia, Tusquets Editores (1997).
- [13] Xu, T., Moore, I. D., and Gallant, J. C., “Fractals, fractal dimensions and landscapes a review,” *Geomorphology* **8**(4), 245–262 (1993).
- [14] So, G.-B., So, H.-R., and Jin, G.-G., “Enhancement of the box-counting algorithm for fractal dimension estimation,” *Pattern Recognition Letters* **98**, 53–58 (2017).
- [15] Talanquer, V. A., [*Fractus, fracta, fractal: fractales, de laberintos y espejos*], Fondo de cultura económica (2011).
- [16] Carbone, A., “Algorithm to estimate the hurst exponent of high-dimensional fractals,” *Physical Review E*. **76**(5), 056703 (2007).

- [17] E. Chandrasekhar, V. P. Dimri, V. M. G., [*Wavelets and Fractals in Earth System Sciences*], CRC Press (2013).
- [18] Silva, L., Saade, D., Sequeiros, G., Silva, A., Paiva, A., Bravo, R., and Conci, A., “A new database for breast research with infrared image,” *Journal of Medical Imaging and Health Informatics* 4(1), 92–100 (2014).